Experimental Study of Overvoltage in the Winding of an Induction Motor Controlled by HF

Mohamed Ali Moussa^{1*}, Bachir Mokhtari², Hamza Sahraoui¹, and Hacene Mellah³

¹LGEER Laboratory, Department of Electrotechnic, University of Chlef 02000, Algeria ²Department of Electrotechnic Niversity of Laghouat 03000, Algeria ³Department of Electrotechnic University of Bouira 10000, Algeria

(Received 29 April 2025, Received in final form 8 August 2025, Accepted 8 August 2025)

The overvoltage created on the supply lines of the driven electric motors can cause harmful damage to the equipment. Sometimes these motors are supplied via unipolar cables, we want by this paper to study the influence of using these cables to supply an induction motor (IM) driven by techniques based on high frequencies on the creation of overvoltage. Two tests are then presented: In the first test, the system is powered directly by a frequency generator without using the single-core cable. In the second test, a single-core cable of different lengths is used between the power supply and the stator of IM. The experimental results obtained at the Algerian Energy and Intelligent Systems Laboratory (LESI), prove that the method proposed for this purpose is quite efficient.

Keywords: harmonics, induction motor, overvoltage, PWM control, HF

1. Introduction

The evolution of power electronics has added to the induction motor (IM) the variable speed drive by associating it with a frequency converter, which is considered an extremely important advantage in industry applications. This advantage has made this IM preferable in the industry because this converter-machine combination has enabled it to achieve dynamic performance comparable to that of a DC motor. This has diversified its applications in wide fields [1].

The operation of the frequency converter is essentially based on the conversion of an alternating voltage at fixed and uncontrollable frequency (voltage of the supply network at 50 Hz) to an alternating voltage at variable and controllable frequencies. This task is performed by the switching of semiconductor switches which are located within a PWM inverter.

To improve the operational efficiency of the convertermachine assembly, the semiconductors used today operate at increasingly higher frequencies. However, these ultrafast switching of the semiconductors used in the inverters generate very restrictive electromagnetic disturbances which will, on the one hand, degrade the bearings of the motor (they cause a transfer of metal between the balls and the bearing tracks (phenomenon of stitching) [2, 3] and on the other hand create significant overvoltage on its windings. The variable speed drives currently available on the market use IGBT power transistors whose switching times are 20 times faster than ten years ago [4, 5]. The very fast voltage fronts and the high switching frequencies of these converters can cause the flow of large HF currents.

In addition, the necessary presence of electric cables - of varying lengths - to connect the various components of the chain: supply network - frequency converter - motor, had, in the event of high switching frequencies, a detrimental effect on the motor winding because these cables also contribute to the amplification of the over-voltage in question [6].

All of these problems can cause a breakdown of the motor windings and therefore its "electrical" destruction or in the least case; these problems cause the used motor to age prematurely.

To represent the IM whose connections of the stator coils are arbitrary, a universal high frequency equivalent circuit model has been proposed by [7-18].

In this paper, we are particularly interested in the

©The Korean Magnetics Society. All rights reserved.

*Corresponding author: Tel: 0213663450831

e-mail: m.alimoussa@univ-chlef.dz

experimental study of the overvoltage, a study which treats their origins and reveals their influences on the aspect and the modulus of the supply voltage of the stator windings.

We have set two objectives:

- 1- To know the influence of the phase length on the overvoltage values;
- 2- To know the cable connection influence on the appearance and value of surges.

In this vision, and after a quick review of cables and overvoltage, we present the tests.

2. Overvoltages

In order to control the induction motor with the best possible performance, variable speed drive is used using a frequency converter (PWM inverter for example). The latter is connected to the motor, on one side, and to the power supply on the other side, by cables of varying lengths.

However, the ultra-fast switching of the power switches (transistors/thyristors) used in frequency converters has resulted in the rise of problems of electromagnetic interference type [8, 9], they create rapid voltage variations (dv/dt) causing the circulation of high frequency currents which propagate between the source (the inverter) and the "victim" (the stator), which causes more or less significant overvoltage at the terminals of the stator windings [10, 19].

Indeed, the overvoltage are due to the capacitive links between the coils themselves and the coils with the mass, these links generated by the high frequency of the signal from the inverter cause overheating which can deteriorate the insulation of the windings, while the HF currents cause a transfer of metal between the balls and the bearing tracks (pitting phenomenon) [11, 12, 20].

3. Equivalent Diagrams of Cable

In the literature we find two models of equivalent diagrams for the cable having only one conductor (unipolar cable): model in π and model in Γ , the two models are equivalent and they are composed by linear quantities. These sizes and the length of the cable are

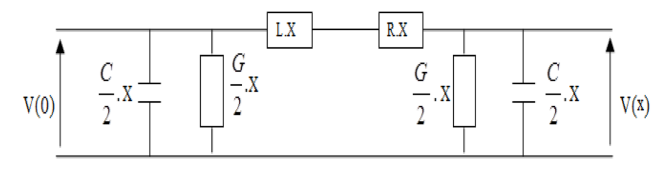


Fig. 1. Section model of a unipolar cable with length X.

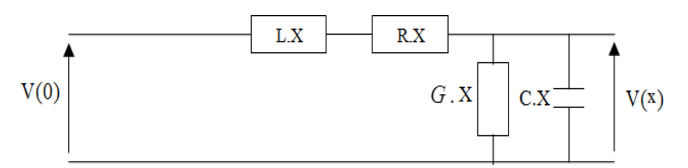


Fig. 2. Section model of a single-core cable with length X.

directly proportional [14, 21-24].

With:

L : longitudinal linear inductance of the cable (H/m)

R: longitudinal linear resistance of the cable (Ω/m)

G: transverse linear conductance of the cable (S/m)

C: transverse linear capacity of the cable (F/m)

X: the length of the cable section (m).

Indeed, the presence of linear capacities in the different models of the equivalent diagrams justifies the contribution of cables to the amplification of overvoltage.

HF calculation of Impedances coils

In Fig. 3, the two-port network is formed by means of frequency-dependent equivalent impedances.

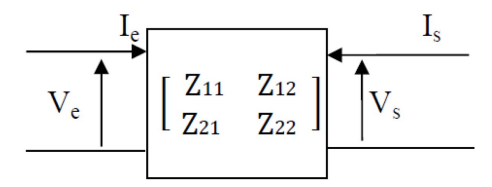


Fig. 3. Impedances of coil two-port network.

Using the input/output voltages, we can easily obtain the characteristic impedances of the two-port network, V_e and V_s [15, 16]:

$$\begin{cases} V_e = Z_{11}I_e + Z_{12}I_s \\ V_s = Z_{21}I_e + Z_{22}I_s \end{cases}$$
 (1)

Or in matrix form:

$$\begin{bmatrix} V_e \\ V_s \end{bmatrix} = \begin{bmatrix} Z_{11} & Z_{12} \\ Z_{21} & Z_{22} \end{bmatrix} \cdot \begin{bmatrix} I_e \\ I_s \end{bmatrix}$$
 (2)

Where the four characteristic impedances are defined as follows:

$$\begin{cases}
Z_{11} = V_{e/I_{e}} & \text{for } I_{s} = 0 \\
Z_{12} = V_{e/I_{s}} & \text{for } I_{e} = 0 \\
Z_{21} = V_{s/I_{e}} & \text{for } I_{s} = 0 \\
Z_{22} = V_{s/I_{s}} & \text{for } I_{e} = 0
\end{cases}$$
(3)

The two-port network in Fig. 3 is symmetrical and reciprocal, so and with:

$$Z_{12} = Z_{21} \text{ and } Z_{11} = Z_{22}$$
 (4)

Calculation Method of the HF Parameters for a Phase Winding

The IM phases in this study are the coils which are connected in series. In Fig. 4, it is shown that at high frequency we find these coils connected in cascade and form a two-port network. The IM coils are not accessible for direct measurement and only its stator coils are. This study demonstrates the calculation of HF parameters of coils based on winding parameters [16, 17, 23-25].

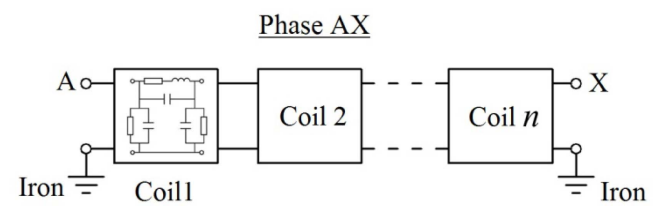


Fig. 4. Two-port networks (winding segments) connected into cascade forming a phase winding of a motor stator.

In order to calculate the parameters of the coils based on measurements made on the stator phases, we developed our calculation method. We assume that all the stator coils are identical, we then have:

$$[T \ 2] = [T_2] = \cdots = [T_n] = T = \begin{bmatrix} T_{11} & T_{12} \\ T_{21} & T_{22} \end{bmatrix}$$
 (5)

Where $[T_1]$, $[T_2]$, \cdots ; $[T_n]$ are the transfers matrices of coils and T_{11} , T_{12} , T_{21} and T_{22} are the coils characteristic parameters of transfer.

We use the association rules in the case of two-port networks formed by a cascade coils, we have:

$$[T_{eq}] = [T_1] \cdot [T_2] \cdots [T_n] = [T]^n.$$

$$(6)$$

The matrix expression of input/output voltages and currents of the two-port network phase, are given by:

$$\begin{bmatrix} V_s \\ I_s \end{bmatrix} = \begin{bmatrix} T_{11} & T_{12} \\ T_{21} & T_{22} \end{bmatrix}^n \cdot \begin{bmatrix} V_e \\ -I_e \end{bmatrix}$$
 (7)

The transfer parameters and the impedance parameters are given by:

$$\begin{bmatrix} T_{11} & T_{12} \\ T_{21} & T_{22} \end{bmatrix} = \begin{bmatrix} \frac{Z_{11}}{Z_{12}} & \frac{\Delta Z}{Z_{12}} \\ \frac{1}{Z_{12}} & \frac{Z_{11}}{Z_{12}} \end{bmatrix} = \frac{1}{Z_{12}} \cdot \begin{bmatrix} Z_{11} & \Delta Z \\ 1 & Z_{11} \end{bmatrix}$$
(8)

Where: $\Delta Z = Z_{11}^2 + Z_{12}^2$.

We deduce then the equivalent transfer matrix:

$$\begin{bmatrix} T_{\text{eq}} \end{bmatrix} = Z_{12}^{-n} \cdot \begin{bmatrix} Z_{11} & \Delta \underline{Z} \\ 1 & Z_{11} \end{bmatrix}^n \tag{9}$$

So, the transfer matrix of the equivalent two-port network of a phase coil is given by:

$$\begin{bmatrix} V_s \\ I_s \end{bmatrix} = Z_{12}^{-n} \cdot \begin{bmatrix} Z_{11} & \Delta Z \\ 1 & Z_{11} \end{bmatrix}^n \cdot \begin{bmatrix} V_e \\ -I_e \end{bmatrix}$$
 (10)

4. Work Environment

In the aim to study the effects of the high frequencies of the supply voltage (PWM inverter for example) of an induction squirrel cage motor on the winding of its stator, we fed the stator windings with a square wave using a frequency generator (FG) with a frequency of 1000 Hz and an amplitude of 10 V. We use a square signal for two reasons:

- It is similar in form to a PWM signal.
- It contains harmonics.

The motor of this study is a three-phase squirrel-cage (3 kW), it is manufactured, on our order, by the "electro-industries" factory of Azazga (Wilaya of Tizi Ouzou), Algeria.

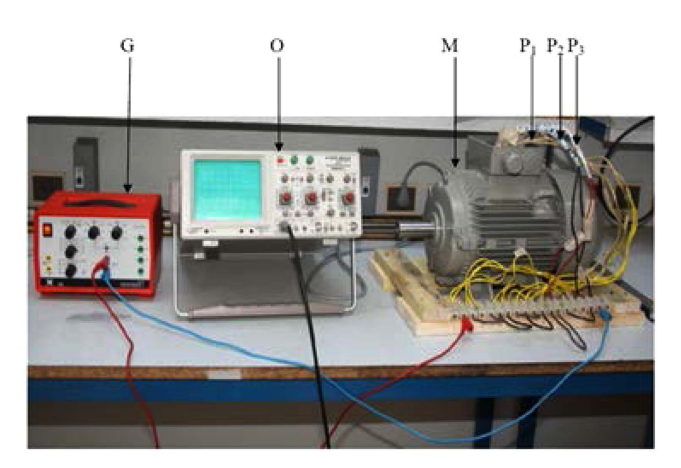


Fig. 5. (Color online) Image of the test bench.

The stator of our motor is made up of three phases: (Fig. 5)

Phase I: phase composed by five open coils able to be connected;

Phase II: ordinary phase;

Phase III: ordinary phase.

The advantage of having open coils lies in the possibility of:

- Connect them in the desired way;
- Measure the voltages and / or overvoltage on their ends.

With:

G is a frequency generator;

O is an oscilloscope with two channels;

M is the IM (3kW);

P1, P2 and P3 are respectively the stator phases (1, 2 and 3).

5. The Experimental Results

For our study, we have subdivided the tests on two tests: the first is without cable and the second is with cable.

A. Tests (without cable)

For this test, we have five tests witch depend to the number of coils and them position in series or parallel.

1. Test with 5 coils in series

We fed phase I (consisting of five open coils) by a square signal produced by the FG (Fig. 6) of module which is worth 10 V, then we measured the voltages and the surge peaks at the terminals of each coil and we calculated their ratios.

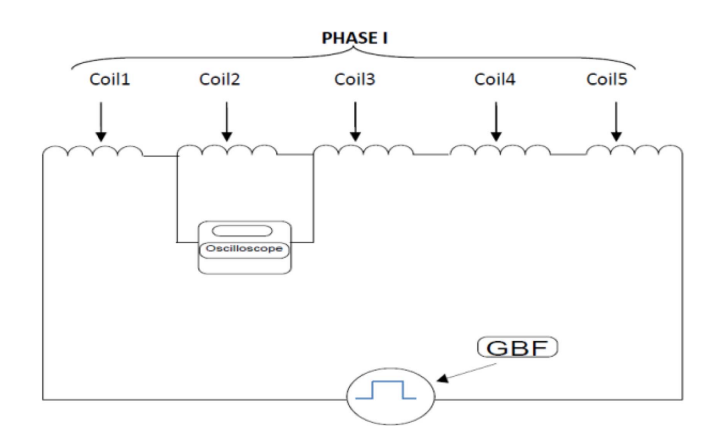


Fig. 6. Diagram of the test with 5 coils in series.

The results of this test are displayed in the table below. We take note that:

U_{aln}: Supply voltage of each coil in volts;

U_{sn}: Overvoltage peak at the terminals of each coil in volts;

n: Coil number.

The results are presented in Table 1 and Fig. 7.

Table 1. Table of the results for 5 coils.

Coils	U _{aln} (V)	U _{sn} (V)	U _{sn} /U _{aln}
1	2	3.20	1.60
2	1.97	2.65	1.34
3	2	2.60	1.30
4	2.01	2.90	1.44
5	1.97	2.80	1.42

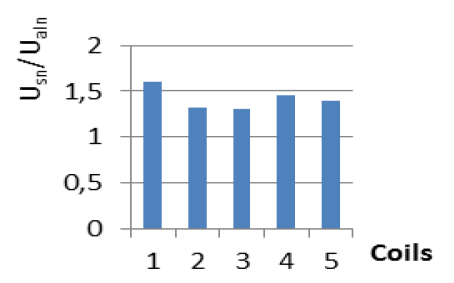


Fig. 7. (Color online) Graph representative of the results for 5 coils.

2. Test with 10 coils in series (phase I and phase II in series).

We put phase I in series with phase II and we feed them with the square signal produced by the FG (as shown in Fig. 8) and we measure the voltages and surge peaks

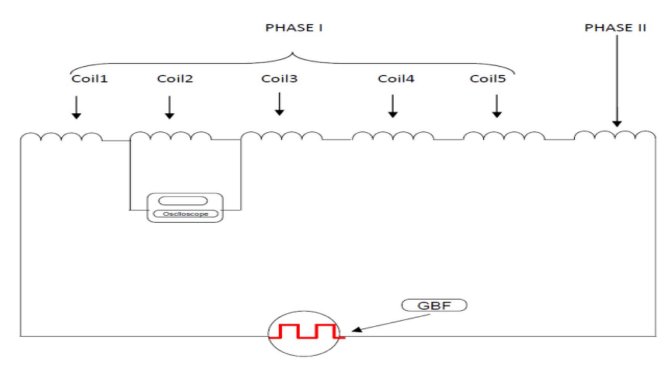


Fig. 8. (Color online) Diagram of the test with 10 coils in series.

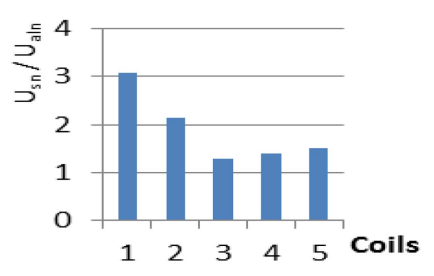


Fig. 9. (Color online) Graph representative of the results for 10 coils.

across each of the five phase I coils.

Phase II is considered the equivalent of five coils in series.

The results are displayed in the table below; they are followed by a graphical representation by Fig. 9 and Table 2.

Table 2. Table of the results for 10 coils.

Coils	U _{aln} (V)	$U_{sn}(V)$	U _{sn} /U _{aln}
1	0.94	2.90	3,07
2	0.93	2.00	2,14
3	0.85	1.10	1,29
4	1.13	1.60	1,41
5	1.10	1.65	1,50

3. Test with 15 coils in series (the three phases in series).

The three phases of the stator are placed in series and are supplied by the same square wave. Measurements of voltage and overvoltage peaks are always taken at the terminals of each of the constituent coils of phase I (Fig. 10).

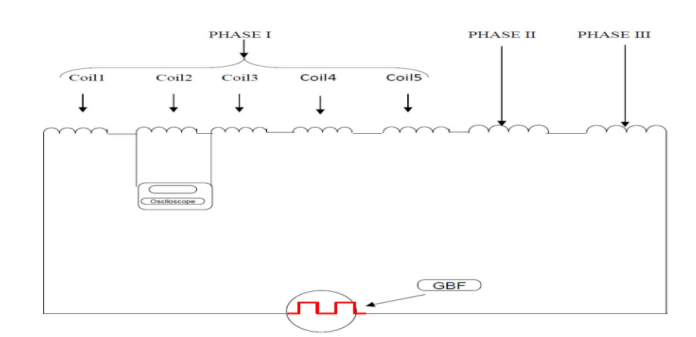


Fig. 10. (Color online) Diagram of the test with 15 coils in series.

The results of this test are displayed in the table below; they are followed by a representative in Fig. 11 and Table 3.

Table 3. Table of the results for 15 coils.

Coils	U _{aln} (V)	$U_{sn}(v)$	U_{sn}/U_{aln}
1	0.55	2.69	4,92
2	0.54	1.59	2,93
3	0.56	0.89	1,58
4	0.66	1.09	1,64
5	0.64	0.99	1,55

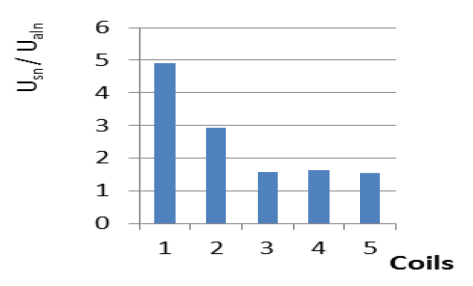


Fig. 11. (Color online) Graph representative of the results for 15 coils.

So, after testing, we have found that:

- The power signal distorts, exhibiting peaks as shown in the Fig. 11;
- According to the results obtained, the length of the winding is proportional to the overvoltage (a simple comparison between the value of the U_{sn}/U_{aln} ratio in the case of a single phase which is equal to 1.6 and the case of three phases in series which is 4.92, confirms this observation.
- 4. Test with phase I in series with the two phases in parallel.

In this test we keep the same number of coils (15 coils) but we reduce the length of the stator windings by connecting phase II in parallel with phase III and the two are put in series with phase I, as illustrated by the diagram in Fig. 12 below.

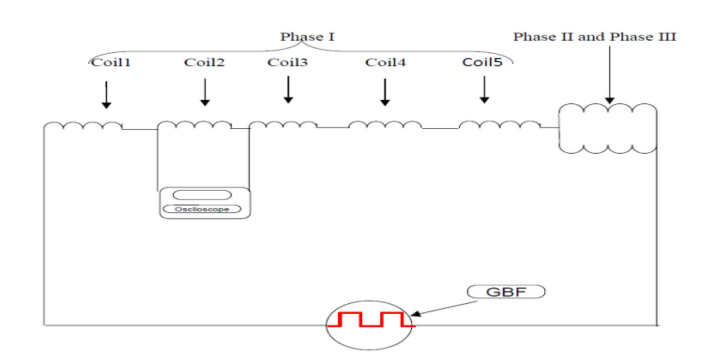


Fig. 12. (Color online) Diagram of the test with parallel tracks.

The results are displayed in the table above, followed by a graphical representation in Fig. 13 and Table 4.

So, using the same number of coils (15 coils) but depending on them in such a way as to have two different lengths of the windings, we find that by using the length of the windings by the use of the parallels we can reduce the overvoltage.

Table 4. Table of the results for parallel channels.

		1	
Coils	U _{aln} (V)	U _{sn} (V)	U _{sn} /U _{aln}
1	0.94	3.45	3,66
2	0.93	2.25	2,41
3	0.85	1.45	1,70
4	1.13	2.25	1,98
5	1.09	2.15	1,96

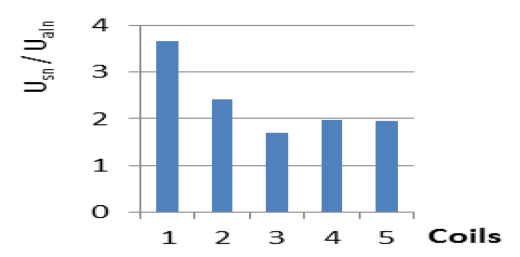


Fig. 13. (Color online) Graph representative of the results for parallel channels.

B. Tests with a cable

In this case, we have taken the effect of an existing cable witch link the power supply and the electrical motor. This montage is illustrated by the Fig. 14 below:

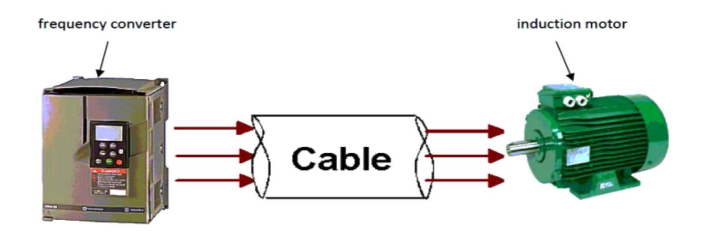


Fig. 14. (Color online) Variable speed drive - cable - motor.

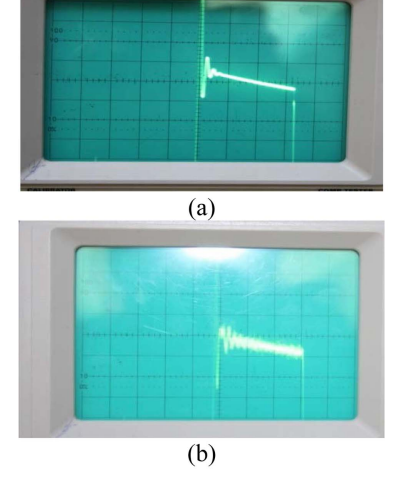


Fig. 15. (Color online) Image from the oscilloscope: (a) Without cable, (b) With cable.

The same previous tests are repeated but inserting, this time, a cable of different lengths between the power supply and the motor stator. Fig. 15 illustrates the appearance of the overvoltage graphs in both cases (without cable and with cable).

The results of the tests carried out, with the values of the largest peaks, are collated in Table 5 below.

Table 5. Influence of Cable Length on Overvoltage Values.

	The pics values of (U _{sn} /U _{aln})		
Number of coils	5 coils	10 coils	15 coils
Cable (7 m)	1.91	3.28	5.64
Cable (13 m)	1.98	3.71	6.03
Cable (20 m)	2	3.76	6.21

The general observation that can be made in the case of using cables of different lengths is summarized by the expression: overvoltage is proportional to the length of the cable, (they can reach more than six times (exactly 6.21) the value of the supply voltage in the case of a 20 m cable).

6. General Analysis and Comparison of Results

Table 6 below shows the most important ratios of surge peaks to supply voltages when using a cable of different lengths or without using it.

Table 6. Comparison of Results.

	The pics values of (U_{sn}/U_{aln})		
Number of coils	5 coils	10 coils	15 coils
Without cable	1.60	3.07	4.92
Cable (7 m)	1.91	3.28	5.64
Cable (13 m)	1.98	3.71	6.03
Cable (20 m)	2	3.76	6.21

So:

- Horizontal reading of the results allows us to say that:
 - As much as the windings are longer, the surge peaks are more important;
 - Surges are mainly localized on the end coils.
- The vertical reading of the results allows us to:
 - Confirm that the use of cables increases surges.
- On the other hand and by comparing the shape of the signal in the two photographs in Fig. 15 above (without cable/with cable), we notice that in the

presence of the cable, the surges take much longer to subside.

7. Conclusion

In this paper, an experimental study was presented to clarify the effect of the presence of a unipolar cable in the power supply of an induction motor. It was a question of checking the appearance of overvoltage in order to limit their peaks which are very dangerous for the motor coils and can destroy them.

The results obtained in this study allowed drawing the following conclusions:

- The overvoltage is not distributed over the entire length of the winding in the same way but they are located on the coils at the end;
- The overvoltage is proportional to the cable length;
- Overvoltage oscillations take longer to subside when using a connection cable;
- The use of parallel tracks contributes to the reduction of overvoltage.

Acknowledgment

We would like to thank very much our colleague, Sayeh KHALFA, teacher-researcher in the English department at the University of Laghouat, for his contribution in writing this paper in English form.

References

- [1] M. S. Toulabi, L. Wang, L. Bieber, S. Filizadeh, and J. Jatskevich, IEEE Transactions on Energy Conversion **34**, 1164 (2019).
- [2] F. Castelli-Dezza, M. M. Maglio, G. Marchegiani, D. F. Ortega, and D. Rosati, The XIX International Conference on Electrical Machines ICEM 2010, Rome, Italy, (2010) pp. 1-6.
- [3] Z. Zhou, Y. Guo, X. Jiang, G. Liu, W. Tang, H. Deng, X. Li, and M. Zheng X. J. Liu, W. Tang, H. Deng, and X. Li, Journal of Marine Science and Engineering 18, 683 (2019).
- [4] D. Roger, E. Napieralska-Juszczak, and K. Komeza, the Journal Open Physics **18**, 619 (2020).
- [5] F. E. Akpoyibo and A. O. Ezechukwu, IRE Journals. 3, 221 (2020).
- [6] D. T. Khanmiri, Ph.D. Dissertation, Overvoltage and Surge Protection in Variable Frequency Drives, Northeas-

- tern University, USA (2020).
- [7] Y. S. Park, J. Magn. 30, 30 (2025).
- [8] L. Wang and J. Jatskevich, Energetika i avtomatika 3, 22 (2013).
- [9] B. Taghia, B. Cougo, H. Piquet, D. Malec, A. Belinger, and J. P. Carayon, Mathematics and Computers in Simulation **158**, 264 (2018).
- [10] S. Bartos, I. Dolezel, J. Necesany, J. Skramlik, and V. Valouch, Acta Electrotechnica & Informatica 8, 3 (2008).
- [11] M. Schinkel, S. Weber, S. Guttowski, W. John, and H. Reichl, Applied Power Electronics Conference and Exposition, Dallas, USA, 1 (2006).
- [12] M. N. Benallal, A. C. Vataev, D. A. TouAn, and T. Nahdi, Izvestia SPGTU"LETI", St Petersburg, Russia. 5, 78 (2011).
- [13] B. Chetate, M. T. Belassel, S. Simard, and R. Beguenane, IEEE Canada Electrical Power Conference, Canada, (2007) pp. 399-404.
- [14] B. Badrzadeh and B. Gustavsen, IEEE Transactions on Power Delivery 27, 746 (2012).
- [15] A. Yazdani and R. Iravani, Voltage-Sourced Converters in Power Systems: Modeling, Control, and Applications, Wiley-IEEE Press, New York (2010) pp. 245-269.
- [16] V. Akhmatov, B. C. Gellert, T. E.McDermott, and W. Wiechowski, 9th Int. Workshop on Large-Scale Integration of Wind Power into Power Systems, Quebec, Canada, 166 (2010).
- [17] B. Gustavsen, IEEE Transactions on Power Delivery. **25**, 770 (2010).
- [18] Z. Zhou, Y. Guo, and X. Jiang, Journal of Marine Science and Engineering 7, 415 (2019).
- [19] D. D'Amato, J. Loncarski, V. Giuseppe Monopoli, F. Cupertino, L. Pio Di Noia, and A. Del Pizzo, Energies 15, 1406 (2022).
- [20] B. Taghia, B. Cougo, H. Piquet, D. Malec, A. Belinger, and J.-P. Carayon, Mathematics and Computers in Simulation 158, 264 (2019).
- [21] J. Tao, Q. Yang, X. Zheng, Y. He, R. Wang, and H. Lv, J. Zhang, Wind Energy **24**, 1501 (2021).
- [22] T. Riouch and C. Nichita, International Journal of Power Electronics and Drive Systems (IJPEDS) **12**, 1422 (2021).
- [23] S. Soeprapto, R. N. Hasanah, and T. Taufik, International Journal of Power Electronics and Drive System (IJPEDS) **10**, 1529 (2019).
- [24] M. N. Abed, O. A. Suhry, and M. A. Ibrahim, International Journal of Power Electronics and Drive Systems (IJPEDS) 13, 200 (2022).
- [25] L. Xie, Z. Xu, P. Su, Y. Li, and L. Chang, J. Magn. **30**, 55 (2025).